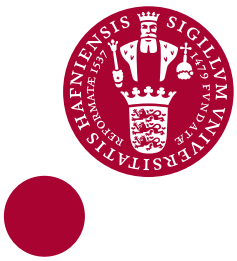

A High-Density Map for Navigating the Human Polycomb Complexome

Hauri, Simon; Comoglio, Federico; Seimiya, Makiko; Gerstung, Moritz; Glatter, Timo; Hansen, Klaus; Aebersold, Ruedi; Paro, Renato; Gstaiger, Matthias; Beisel, Christian

Published in:
Cell Reports

DOI:
10.1016/j.celrep.2016.08.096

Publication date:
2016

Document version
Publisher's PDF, also known as Version of record

Resource

Cell Reports

A High-Density Map for Navigating the Human Polycomb Complexome

Graphical Abstract

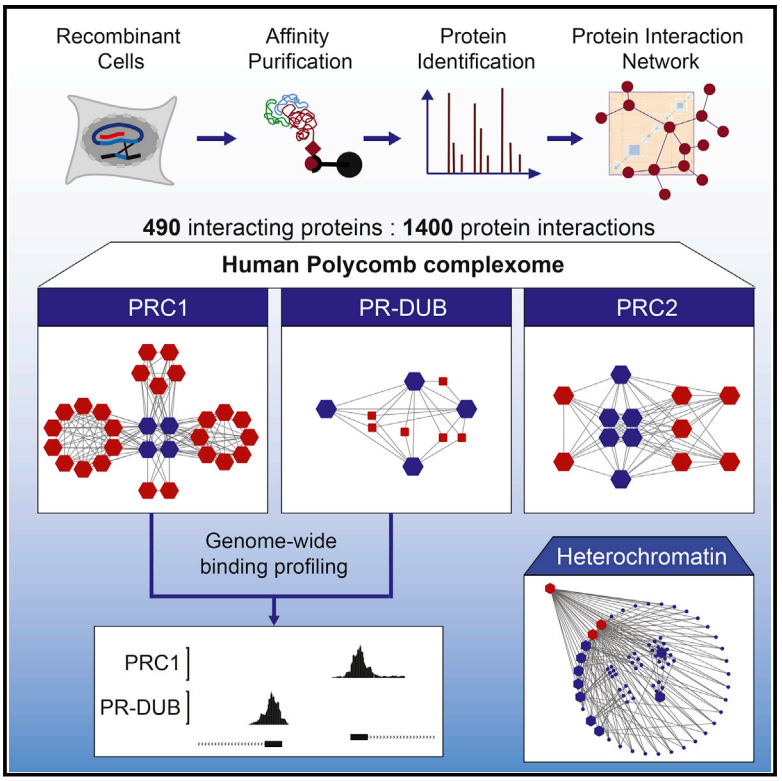

Authors

Simon Hauri, Federico Comoglio, Makiko Seimiya, ..., Renato Paro, Matthias Gstaiger, Christian Beisel

Correspondence

matthias.gstaiger@imsb.biol.ethz.ch (M.G.), christian.beisel@bsse.ethz.ch (C.B.)

In Brief

Polycomb group (PcG) proteins mediate gene silencing and epigenetic memory in higher eukaryotes. By systematically mapping the human PcG complexome, Hauri et al. resolve Polycomb subcomplexes at high resolution and identify two human PRC2 and two PR-DUB complexes. Furthermore, genomic profiling reveals segregation of PRC1 and PR-DUB target genes.

Highlights

- 1,400 high-confidence interactions reveal the modular organization of human PcG proteins
- Detailed dissection of PRC1 and PRC2 subcomplexes
- Two human PR-DUB complexes contain the glycosyltransferase OGT1
- PR-DUB and PRC1 bind largely distinct sets of target genes

Accession Numbers

GSE51673

Hauri et al., 2016, Cell Reports *17*, 583–595
October 4, 2016
http://dx.doi.org/10.1016/j.celrep.2016.08.096

Cell Reports
Resource

A High-Density Map for Navigating the Human Polycomb Complexome

Simon Hauri,[1,2,7,8] Federico Comoglio,[3,7,9] Makiko Seimiya,[3] Moritz Gerstung,[3,10] Timo Glatter,[1,11] Klaus Hansen,[4] Ruedi Aebersold,[1,5] Renato Paro,[3,6] Matthias Gstaiger,[1,2,*] and Christian Beisel[3,12,*]

[1]Department of Biology, Institute of Molecular Systems Biology, ETH Zürich, 8093 Zürich, Switzerland
[2]Competence Center Personalized Medicine UZH/ETH, 8044 Zürich, Switzerland
[3]Department of Biosystems Science and Engineering, ETH Zürich, 4058 Basel, Switzerland
[4]Biotech Research and Innovation Centre (BRIC) and Centre for Epigenetics, University of Copenhagen, 2200 Copenhagen, Denmark
[5]Faculty of Science, University of Zürich, 8057 Zürich, Switzerland
[6]Faculty of Sciences, University of Basel, 4056 Basel, Switzerland
[7]Co-first author
[8]Present address: Department of Clinical Sciences, Lund University, 221 00 Lund, Sweden
[9]Present address: Department of Haematology, Cambridge Institute for Medical Research and Wellcome Trust/MRC Cambridge Stem Cell Institute, University of Cambridge, CB2 0XY Cambridge, UK
[10]Present address: European Bioinformatics Institute (EMBL-EBI), Wellcome Genome Campus, CB10 1SD Hinxton, UK
[11]Present address: Mass Spectrometry and Proteomics, Max Planck Institute for Terrestrial Microbiology, 35043 Marburg, Germany
[12]Lead Contact
*Correspondence: matthias.gstaiger@imsb.biol.ethz.ch (M.G.), christian.beisel@bsse.ethz.ch (C.B.)
http://dx.doi.org/10.1016/j.celrep.2016.08.096

SUMMARY

Polycomb group (PcG) proteins are major determinants of gene silencing and epigenetic memory in higher eukaryotes. Here, we systematically mapped the human PcG complexome using a robust affinity purification mass spectrometry approach. Our high-density protein interaction network uncovered a diverse range of PcG complexes. Moreover, our analysis identified PcG interactors linking them to the PcG system, thus providing insight into the molecular function of PcG complexes and mechanisms of recruitment to target genes. We identified two human PRC2 complexes and two PR-DUB deubiquitination complexes, which contain the O-linked N-acetylglucosamine transferase OGT1 and several transcription factors. Finally, genome-wide profiling of PR-DUB components indicated that the human PR-DUB and PRC1 complexes bind distinct sets of target genes, suggesting differential impact on cellular processes in mammals.

INTRODUCTION

Cell division requires faithful replication of the genome and restoration of specific chromatin states that form the basis of epigenetic memory (Sarkies and Sale, 2012). Polycomb group (PcG) proteins were originally identified in *Drosophila melanogaster* as stably maintaining the repressed state of homeotic genes throughout development and are key players in this process. Numerous studies have since established a central role for PcG proteins in the dynamic control of hundreds of targets in metazoans, including genes affiliated to fundamental signaling pathways (Ringrose, 2007). Biological processes regulated by PcG proteins encompass cell differentiation, tissue regeneration, and cancer cell growth (Jaenisch and Young, 2008; Maurange et al., 2006; Sparmann and van Lohuizen, 2006).

The PcG system consists of multimeric repressive protein complexes containing distinct chromatin modifying activities, which impact transcriptional regulation by modulating chromatin structures. In *Drosophila*, five distinct PcG complexes displaying different biochemical functions have been reported. The Polycomb repressive complex (PRC) 2 contains enhancer of zeste, which trimethylates lysine 27 of histone H3 (H3K27me3) (Cao et al., 2002; Müller et al., 2002), while the PRC1 subunit Polycomb provides binding specificity to H3K27me3 through its chromo-domain (Fischle et al., 2003; Min et al., 2003). PRC1 also contains the dRing protein, which catalyzes the mono-ubiquitination of histone H2A on lysine 118 (H2AUb1), thereby blocking RNA polymerase II activity (de Napoles et al., 2004; Stock et al., 2007; Wang et al., 2004). The Pleiohomeotic (Pho, *Drosophila* homolog of mammalian YY1) repressive complex PhoRC combines DNA- and histone tail-binding specificities (Klymenko et al., 2006), the PRC1-related dRing-associated factors complex (dRAF) contains the H3K36-specific histone demethylase dKDM2 (Lagarou et al., 2008), and the Polycomb repressive deubiquitinase (PR-DUB) targets H2AUb1 (Scheuermann et al., 2010).

Although the core components of *Drosophila* PcG complexes seem fixed, we and others have shown that they can be co-purified with different sets of accessory proteins, thus increasing the diversity of the PcG system (Furuyama et al., 2004; Klymenko et al., 2006; Saurin et al., 2001; Strübbe et al., 2011). Epigenomic profiling has revealed that distinct PcG complexes target largely overlapping gene sets in *Drosophila*, and mechanistic details of PcG recruitment to target genes are beginning to emerge (Beisel

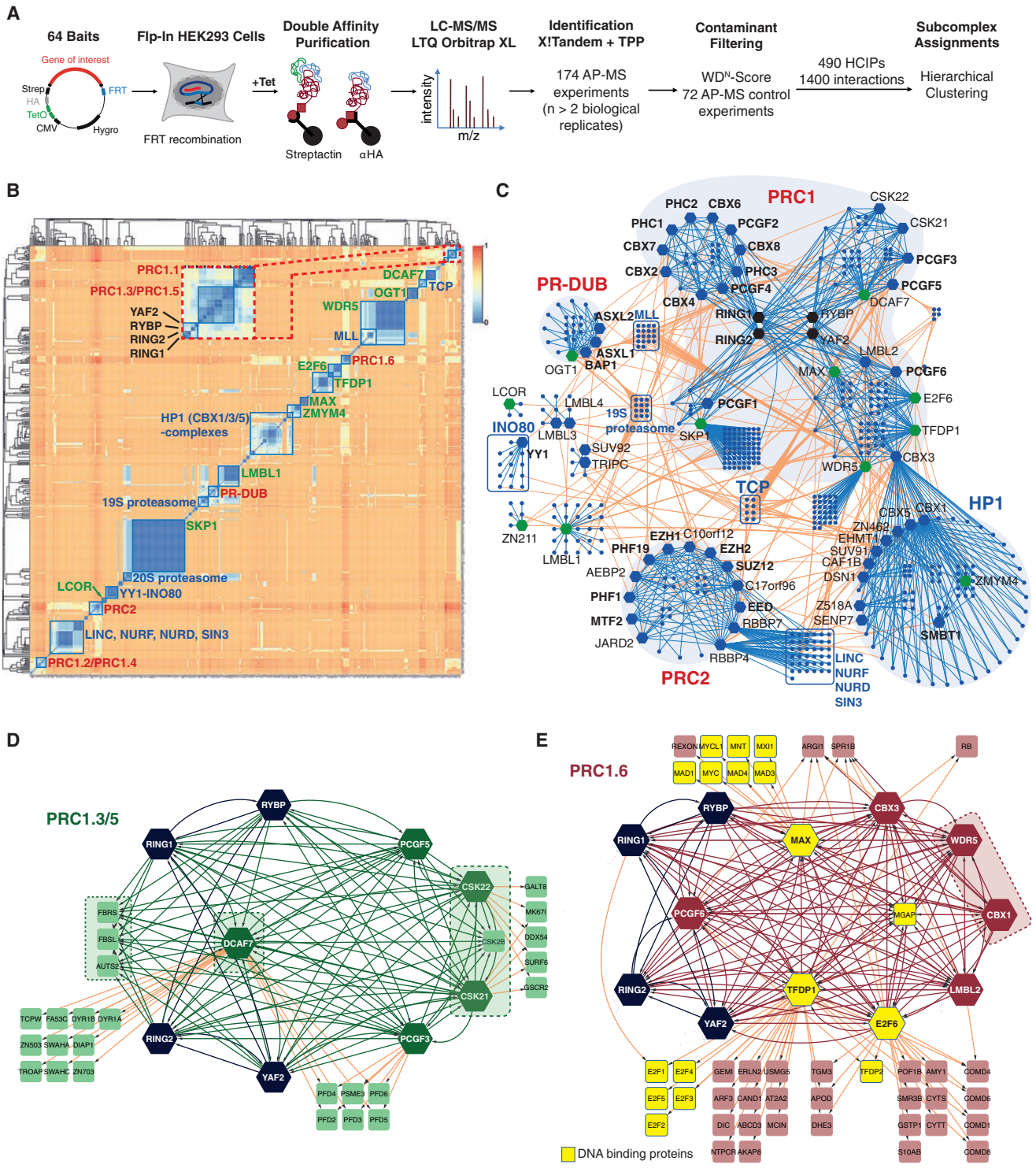

Figure 1. Systematic Profiling of Human PcG Protein Complexes

(A) Workflow for native protein complex purifications from Flp-In HEK293 T-REx cells. Open reading frames of 64 bait proteins were cloned into an expression vector containing a tetracycline inducible CMV promoter, Strep-HA fusion tag, and FRT sites. The proteins were affinity purified from whole cell extracts of isogenic cell lines, trypsinized, and identified by tandem mass spectrometry on an LTQ Orbitrap XL. HCIPs were hierarchically clustered to infer protein complex compositions. (B) Hierarchical clustering of HCIPs. Clusters of PcG and non-PcG complexes are labeled in red and blue, respectively. The inset shows the location of PRC1.1, PRC1.3/PRC1.5, and the four core proteins RYBP/YAF2 and RING1/2. The clusters defined by single baits are indicated in green. Spearman's rank correlation coefficient based dissimilarities are color coded as indicated (top right).

(legend continued on next page)

and Paro, 2011; Enderle et al., 2011; Oktaba et al., 2008; Scheuermann et al., 2010; Schuettengruber et al., 2009).

In contrast, the mammalian PcG system is less well defined and appears to be significantly more complex. Each *Drosophila* PcG subunit has up to six human homologs, which combinatorially assemble in different complexes (Gao et al., 2012; Margueron et al., 2008; Shen et al., 2008). The six homologs of the *Drosophila* PRC1 core protein Psc, PCGF1–6, purify together with RING2 (RNF2), the homolog of dRing, in different complexes named PRC1.1–PRC1.6, and each of them associates with specific additional components (Gao et al., 2012; Sánchez et al., 2007). These PRC1 complexes are further distinguished by the mutually exclusive presence of RYBP or a chromo-domain-containing CBX protein. There are five different CBX proteins displaying differential affinities for lysine-methylated histone H3 tails and RNA (Bernstein et al., 2006) that have been linked to PRC1. In contrast, the absence of a chromo-domain within RYBP suggests that recruitment of CBX and RYBP containing PRC1 complexes might be mediated by H3K27 methylation or be independent of it, respectively. Indeed, recent work showed that the histone demethylase Kdm2b targets PRC1.1 (the dRAF analog) via direct binding to unmethylated CpG islands (Farcas et al., 2012; He et al., 2013; Wu et al., 2013). Incorporation of RING2 in optional PCGF complexes not only leads to differential recruitment to chromatin, but also differentially regulates its enzymatic activity (Farcas et al., 2012; Gao et al., 2012; Morey et al., 2012; Tavares et al., 2012; Wu et al., 2013).

Similar to PRC1, the histone methyltransferase (HMT) activity of PRC2 is potentially modulated by accessory components such as the Polycomb-like homologs PHF1, PHF19, and MTF2 (Hunkapiller et al., 2012; Sarma et al., 2008). Additional DNA binding interaction partners like JARD2 (JARID2) and AEBP2 might mediate recruitment of the complexes to chromatin (Kim et al., 2003; Pasini et al., 2010; Peng et al., 2009; Shen et al., 2009). Likewise, several interaction partners with chromatin and DNA binding activity have been identified for BAP1 and ASXL1/2, the human homologs of the *Drosophila* PR-DUB subunits (Baymaz et al., 2014; Dey et al., 2012; Ji et al., 2014). However, whether the PRC2 core, consisting of EED, SUZ12, and EZH2, and the PR-DUB core, consisting of BAP1 and ASXL1 (and/or ASXL2), simultaneously interact with all of these components or whether distinct complexes co-exist remains unknown. Moreover, mammalian PhoRC has not been identified to date.

Understanding PcG-mediated epigenetic regulation in mammals requires a detailed understanding of the dynamic assembly of PcG complexes. A required step toward this goal is the exhaustive definition of the composition of individual PcG complexes including all accessory proteins, which likely convey distinct functional effects. Here, we present a systematic and comprehensive high-density map outlining the modular organization of the human PcG system using a sensitive double-affinity purification and mass spectrometry (AP-MS) method (Glatter et al., 2009; Varjosalo et al., 2013). The resulting map of 1,400 interactions and 490 proteins considerably refines the topology of the human PRC1 and PRC2 network, including their relation with the heterochromatin silencing system, and uncovers additional interaction partners. Furthermore, we determined the composition of the human PR-DUB. We found that this highly diverse complex contains MBD proteins, FOXK transcription factors, and OGT1 (OGT), an O-linked N-acetylglucosamine (O-GlcNAC) transferase implicated in PcG silencing in *Drosophila* (Gambetta et al., 2009). Finally, chromatin profiling of PR-DUB components and comparison with chromatin maps of PcG proteins indicate that in contrast to *Drosophila*, PRC1 and PR-DUB regulate distinct sets of genes in human cells.

RESULTS AND DISCUSSION

Systematic Mapping of the Human PcG Interaction Proteome

To investigate the human PcG protein interaction network, we applied a systematic proteomics approach, based on our previously reported AP-MS protocol in HEK293 cells (Glatter et al., 2009). The method employs Flp-In HEK293 stable cell lines expressing Strep-HA-tag fusion proteins upon tetracycline induction (Figure 1A). Initially, we selected 28 PcG proteins homologous to *Drosophila* core complex components and performed AP-MS experiments using these proteins as "primary baits" (Figure S1A). Then, based on the observed interaction data from this set, we chose 36 additional "secondary bait" proteins (Figure S1A; Table S1). After double-affinity purification, bait-associated proteins (preys) were identified by liquid chromatography (LC) tandem MS/MS (Figure 1A). At least two biological replicates were measured for each bait protein, for a total of 174 AP-MS measurements. Proteins were identified using the X!Tandem search tool to match mass spectra to peptides, and the Trans-Proteomic Pipeline (TPP) to map peptides to proteins, at a false discovery rate (FDR) of less than 1% (Craig and Beavis, 2004; Deutsch et al., 2010). The resulting raw data set contained 930 proteins exhibiting 9,856 candidate interactions.

To efficiently discriminate biologically relevant interaction partners from contaminant proteins, we devised a stringent filtering procedure based on both WD^N-score (Behrends et al., 2010) and average enrichment over control purifications for each bait-prey pair (Tables S2 and S3). Interacting proteins with WD^N-score >1 and a control ratio >10 were considered high confidence interacting proteins (HCIPs). This filtering strategy retained 490 HCIPs, encompassing 1,400 (1,193 unidirectional and 207 reciprocal) interactions. Our data set is characterized by an average of 21.9 HCIPs per bait protein, with 75% of interactions that have not yet been annotated in the IntAct database (Figure S1B).

To evaluate the specificity and sensitivity of our AP-MS data, we considered the two bait proteins exhibiting the highest number of HCIPs, SKP1 (79 HCIPs) and WDR5 (73), and performed a cross-validation with literature-based reports. SKP1 serves as

(C) Protein-protein interaction network of clustered interaction data. The blue lines indicate interactions between proteins within the same cluster. Enlarged hexagon-shaped nodes correspond to the baits used in this study.
(D and E) High-density interaction maps of PRC1.3/PRC1.5 (D) and PRC1.6 (E). The new subunits are highlighted by dashed boxes. The hexagon shaped nodes represent baits; squares: identified HCIPs not used as baits in this study. Black nodes: common core subunits; yellow nodes: DNA binding proteins.

an adaptor for F-Box proteins and CUL1 and confers enzymatic specificity. Out of 79 HCIPs, our SKP1 purifications identified 42 F-Box proteins (Figure S1C). Furthermore, a previous AP-MS study investigating the interaction partners of WDR5 (Cai et al., 2010) identified a set of 21 proteins associating with this scaffold protein, which takes part in the assembly of several chromatin-regulating complexes (reviewed in Migliori et al., 2012). Notably, while we were able to recall 76% of previously reported interaction partners, our experiments identified an additional set of 48 proteins (Figure S1D) co-purifying with WDR5 and encompassing MLL complexes, the NSL complex, the ADA2/GCN5/ADA3 transcription activator complex, mTORC2 components RICTR (RICTOR) and SIN1 (MAPKAP1), and the Polycomb repressive complex PRC1.6 (Figure S1E).

Hierarchical Clustering Assigns HCIPs to PcG Complexes

To determine the topology of our protein interaction network, we performed hierarchical clustering of HCIPs using a rank-based correlation dissimilarity measure (see the Supplemental Information for details). Clustering revealed a modular organization built upon the three major PcG assemblies PRC1, PRC2, and PR-DUB and HP1-associated complexes (Figures 1B and 1C).

PRC1 represents the most elaborate and heterogeneous assembly, containing four groups of complexes defined by the six PCGF proteins: PRC1.1 (PCGF1), PRC1.2/PRC1.4 (PCGF2/4), PRC1.3/PRC1.5 (PCGF3/5), and PRC1.6 (PCGF6). Among these PRC1 assemblies, PRC1.6 further provides links to the heterochromatin control system via the HP1 chromobox proteins CBX1 and CBX3.

Although analysis of the PRC1 topology has been recently reported in studies concentrating on specific subunits in various cellular systems (Gao et al., 2012; van den Boom et al., 2013, 2016), our systematic high-density interaction data allowed us to further refine the composition of the PRC1 module. In the following discussion, we focus on the main aspects of this refinement, which are illustrated in Figures 1B–1E and S3 and detailed in Table S2.

All four PRC1 assemblies share a common core encompassing the E3 ubiquitin ligases RING1 and RING2 and—with exception of PRC1.2/PRC1.4—RYBP and YAF2. Interestingly, PCGF2/4 also interact with RYBP and YAF2. As these proteins do not share any additional interaction partner besides RING1/2 (Figure S3B), RYBP/YAF-PCGF2/4-RING complexes might correspond to transient products before specific canonical and non-canonical PRC1 holo-complexes assemble. Furthermore, we did not detect any protein stably associating with all canonical PRC1 core members (RING1/2, PHC1–3, CBX2/4/6/7/8, and PCGF2/4). However, we identified NUFP2 (nuclear fragile X mental retardation interacting protein 2, NUFIP2), a putative RNA binding protein exhibiting interactions with CBX2/6/7, PHC3, and PCGF4, as a PRC1 interacting protein (Figure S3B).

The PRC2 complex is separated from both PRC1 and HP1 (Figure 1C). The two characteristic histone binding proteins RBBP4 and RBBP7 not only belong to the PRC2 core along with SUZ12, EED, and EZH1/2, but also partake in other protein complexes such as LINC, NURF, NURD, and SIN3 (Figure S2A).

Finally, we identified the PcG complex PR-DUB defined by ASXL1/2 and BAP1 (Figure 1C). Our clustering analysis also revealed complexes such as the TCP chaperonin and the proteasomal lid, that primarily consist of prey proteins (Figure 1B). Of note, several proteins belonging to MLL complexes share interactions between PRC1.3/PRC1.5 (CSK21/22 [CSNK2A1/2]), PRC1.6 (WDR5), and PR-DUB (OGT1) (Figure 1C). In contrast, interaction modules centered on LMBL1/3/4 (L3MBTL1/3/4), SUV92 (SUV39H2) and TRIPC (TRIP12), LCOR, ZN211 (ZNF211), and YY1 (the homolog of *Drosophila* Pho) are more disconnected and tend to be sparse (Figures 1C, 2D, S2B, and S2C). Although YY1 interacts with all subunits of the INO80 chromatin remodeling complex, our AP-MS data do not unveil an equivalent of the *Drosophila* PhoRC complex (Figure S2B). However, except for PhoRC, we were able to reconstitute all mammalian equivalents of *Drosophila* PcG protein assemblies in detail.

WD40 Domain Proteins DCAF7 and WDR5 Are Central Scaffolding Proteins for PRC1.3/PRC1.5 and PRC1.6

The WD40 domain protein DCAF7 has been implicated in skin development and cell proliferation by interacting with DIAP1 (DIAPH1) and the dual-specificity tyrosine phosphorylation-regulated kinase DYR1A (DYRK1A) (Miyata and Nishida, 2011). Intriguingly, DCAF7 co-purified with CBX4/6/8, RING1/2, RYBP/YAF2, and PCGF3/5/6, indicating that the protein is deeply embedded in the PRC1 module. As recent studies also reported interactions between DCAF7 and members of the canonical PRC1 complex, as well as PCGF3/5/6 (Dietrich et al., 2012; El Messaoudi-Aubert et al., 2010; Sánchez et al., 2007; Vandamme et al., 2011), we performed DCAF7 purifications to test whether the protein is indeed a universal subunit of several different RING1/2-containing complexes.

Our DCAF7 AP-MS revealed reciprocal interactions with all bait proteins within a cluster centered on PCGF3 and 5 (Figures 1D and S3C), with no relation to the other PCGF complexes. Moreover, we identified DYR1A/B, DIAP1, the zinc finger transcription factors (ZNFs) ZN503 (ZNF503) and ZN703 (ZNF703), and the ankyrin-repeat proteins SWAHA (SOWAHA) and SWAHC (SOWAHC) as an unrelated module interacting with DCAF7 (Figure 1D). This result suggests that DCAF7 acts as a scaffold for several different protein complexes.

As for RING1/2, RYBP/YAF2, and PCGF3/5, DCAF7 interacts with the tetrameric casein kinase 2 (CSK2) and the three paralogs AUTS2, FBRS, and FBSL (FBRSL1). Therefore, to further refine the PRC1.3/PRC1.5 subnetwork, we performed AP-MS experiments using the catalytic casein kinase subunits CSK21 and CSK22. Our results confirmed the topology of the PCGF3/5-DCAF7 assemblies and identify CSK2 and three uncharacterized proteins within the AUTS2 family as part of PRC1.3/PRC1.5 (Figures 1D and S3C).

The protein PCGF6 was initially purified together with the transcription factors E2F6, MAX, TFDP1, and MGAP (MGA), as well as RING1/2, YAF2, LMBL2, CBX3, and the HMTs EHMT1 and EHMT2, an assembly denoted as E2F6.com (Ogawa et al., 2002). However, subsequent studies were unable to recover the entire (holo) E2F6.com (Gao et al., 2012; Qin et al., 2012; Sánchez et al., 2007; Trojer et al., 2011). Moreover, recent data

suggest that PCGF6 and RING2 might interact with the WD40 domain protein WDR5 (Gao et al., 2012). We therefore decided to revisit the topology of the PCGF6-E2F6 network and to probe WDR5 connectivity by adding MAX, TFDP1, E2F6, LMBL2, CBX3, EHMT2, and WDR5 to our bait collection. Our AP-MS experiments unraveled a high-density network including reciprocal interactions between all but one (EHMT2) baits within this set (Figures 1E and S2C), thus demonstrating that the major PRC1.6 complex resembles E2F6.com. In addition, MGAP, MAX, TFDP1, and E2F6 purifications revealed a rich set of transcription factors that can heterodimerize with these proteins, but that are not part of PRC1.6 as they did not connect to any other component thereof (Figure 1E).

Recently, WDR5 was also reported to be part of the non-specific lethal (NSL) complex and to form a trimeric complex with RBBP5 and ASH2L, which stimulates the H3K4-specific activity of the SET1 HMT family members SET1A (SETD1A), SET1B (SETD1B), and MLL1 (Cai et al., 2010; Dou et al., 2006; Wysocka et al., 2006; Zhang et al., 2012). Interestingly, while we recalled these interactions, we additionally detected reciprocal interactions of WDR5 with all PRC1.6 subunits, thus demonstrating that WDR5 is a universal component of activating and repressing chromatin-modifying complexes.

Taken together, our results identify the WD40 domain proteins DCAF7 and WDR5 as subunits of PRC1.3/PRC1.5 and PRC1.6, respectively. Importantly, recent studies suggested that the diversity of PRC1 complexes might be specified by binding preferences of PCGF proteins, which are mediated by their RING finger- and WD40-associated ubiquitin-like (RAWUL) C-terminal domain (Junco et al., 2013; Sanchez-Pulido et al., 2008). For example, the PCGF1 and PCGF2/4 RAWUL domains selectively interact with BCOR/BCORL (BCORL1) and PHC proteins, respectively (Junco et al., 2013). Based on these analyses, and since WD40 domain-containing proteins often scaffold multisubunit complexes (Migliori et al., 2012), we propose that DCAF7 and WDR5 may serve as central scaffolding proteins for PRC1.3/PRC1.5 and PRC1.6.

CBX1 Partitions in Several Distinct Heterochromatin Complexes Including PRC1.6

In contrast to previous studies, which reported CBX3 as the only heterochromatin protein within E2F6.com, we unexpectedly detected CBX1 in all our PRC1.6-related pull-down experiments. To corroborate this finding, we performed AP-MS experiments with CBX1, using the constitutive heterochromatin protein CBX5 as control. Our results indicate that while CBX5 is disconnected from the PCGF6-E2F6 network, components therein interact with CBX1 (Figure 1E; Table S2). Furthermore, they validate interactions of EHMT2 with CBX1 and CBX3 and, to our surprise, separate EHMT2 and EHMT1 from PRC1.6, suggesting a separate complex containing CBX1/3, EHMT1/2, and ZNF proteins, as well as the KRAB-ZNF interacting and co-repressor protein TIF1B (TRIM28) (Figure S4A).

Given that the PcG and heterochromatin silencing systems are functionally and molecularly related through PcG CBX2/4/6/7/8 and HP1 CBX1/3/5 proteins (reviewed in Beisel and Paro, 2011), we further explored the CBX1/3/5 core of our network, seeking for potential connections between these two systems. This survey led to a refined topology of CBX1/3/5-containing complexes and identified new interacting partners (Figures S4B–S4E). However, we did not detect additional connections to PcG proteins, suggesting limited direct cross-talk between protein components of the two silencing systems.

The PRC2 Core Partitions into Two Different Classes of Complexes

Although the functional core complex of PRC2 is composed of SUZ12, EED, RBBP4/7, and either EZH1 or EZH2, additional accessory proteins have been identified which may regulate the H3K27 HMT activity of the complex and its recruitment to chromatin (Alekseyenko et al., 2014; Kalb et al., 2014; Margueron and Reinberg, 2011). However, how these proteins are organized within PRC2 or whether they assemble into independent PRC2 subcomplexes remains largely unresolved. To elucidate the topological organization of PRC2 complexes, we performed AP-MS experiments using 14 reported PRC2-associated proteins (Figure S1A).

Hierarchical clustering analysis assigned all PRC2 baits to a single cluster exhibiting high intra-cluster correlations (Figures 1B and 2A) and forming a high-density interaction network (Figure 2B). However, when reciprocal interactions were taken into account, our data revealed two fundamental alternative assemblies linked to the PRC2 core, the first defined by AEBP2 and JARD2 and the second by the mutually exclusive binding of one of the three Polycomb-like homologs (PCLs) PHF1, PHF19, and MTF2, respectively (Figure 2B).

Taken together, our results identify two structurally distinct classes of PRC2 complexes. We therefore propose a consistent nomenclature for PRC2, in which we refer to the two PRC2 wings as PRC2.1 (mutually exclusive interaction of PHF1, MTF2, or PHF19) and PRC2.2 (simultaneous interaction of AEBP2 and JARD2). AEBP2 and JARD2 can directly bind to DNA and have been implicated in the recruitment of PRC2 and modulation of its enzymatic activity (Kalb et al., 2014; Kim et al., 2009; Pasini et al., 2010). Interestingly, depletion of JARD2 has only a mild effect on global H3K27 methylation levels, suggesting that PRC2.1 might be primarily responsible for maintaining H3K27me3 patterns genome wide.

C10ORF12 and C17ORF96 Are Mutually Exclusive Subunits of the Polycomb-like Class of PRC2 Complexes

Our purifications of the PRC2 core members and PCLs identified two largely uncharacterized proteins, C10ORF12/LCOR and C17ORF96 (Figure 2B), which have been recently discovered as potential PRC2 components and co-localize on chromatin with EZH2 (Alekseyenko et al., 2014; Maier et al., 2015; Smits et al., 2013; Zhang et al., 2011). Their placement within the PRC2 topology and their functional role remained unknown, however.

Purifications of C17ORF96 confirmed all interactions with PCLs (Figure 2B), and computational sequence analysis revealed that C17ORF96 is present in all vertebrate genomes. Interestingly, BLAST identified a single protein related to C17ORF96 in the human genome, the SKI/DAC domain-containing protein 1 (SKDA1 [SKIDA1]) (Figure S5A). SKDA1 belongs to the DACH family, which is defined by the presence of

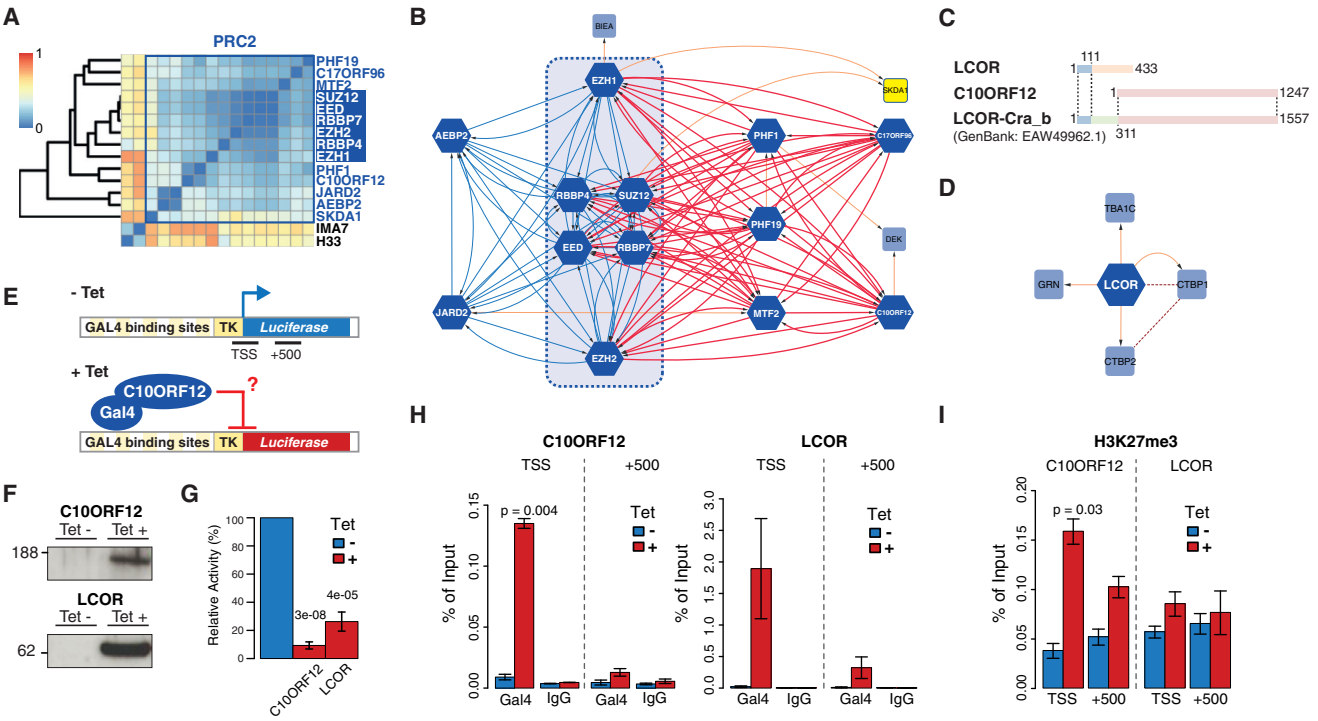

Figure 2. High-Resolution Interaction Analysis Unravels Two Structurally Distinct Classes of PRC2 Complexes

(A) Excerpt of Figure 1B showing the PRC2 cluster.

(B) Interaction map of PRC2 components. The PRC2 core is highlighted by a dashed box. The reciprocal interactions defining the two classes of PRC2 complexes are indicated in red (PRC2.1) and blue (PRC2.2) edges. Orange edges: non-reciprocal interactions.

(C) Schematic representation of alternative protein isoforms of LCOR and C10ORF12. The numbers indicate amino acid positions.

(D) LCOR interaction map. Orange edges, interactions defined in this study; dashed edges, published interactions.

(E) Schematic representation of the employed luciferase reporter system. The amplicons (TSS, +500) used for ChIP-qPCR analysis are indicated.

(F) Anti-Gal4 western blot showing the expression of Gal4-C10ORF12 and Gal4-LCOR upon tetracycline induction.

(G) Luciferase activity of tetracycline-induced Gal4-C10ORF12 and Gal4-LCOR expressing cells, normalized to uninduced cells. The values are mean ± SD and p values are from a two-sided t test (n = 7).

(H) Anti-Gal4 ChIP-qPCR analysis showing localization of C10ORF12 and LCOR to the reporter TSS.

(I) Anti-H3K27me3 ChIP-qPCR analysis at the reporter TSS upon C10ORF12 and LCOR expression. The values are mean ± SD and p values are from a two-sided t test (n = 3).

a SKI/SNO/DAC domain of about 100 amino acids, and is involved in various aspects of cell proliferation and differentiation (Caubit et al., 1999; Wu et al., 2007). However, C17ORF96 lacks the SKI/SNO/DAC domain, and its homology to SKDA1 is restricted to the C terminus (53% sequence identity within the last 60 amino acids) (Figures S5A and S5B), suggesting that this region encodes a hitherto uncharacterized protein domain. Interestingly, SKDA1 also interacts with EZH1 and SUZ12 (Figure 2B), suggesting that this putative C-terminal domain mediates the interaction of C17ORF96 and SKDA1 with the PRC2 core.

Initial analysis of C10ORF12, the second uncharacterized protein highly connected to the PRC2 core, identified peptides that ambiguously mapped to two distinct UniProt proteins, LCOR and C10ORF12 (Figures S5C–S5E). These two proteins are encoded by the same genomic locus. Indeed, in contrast to the UniProt database, GenBank contains the ligand-dependent co-repressor, isoform CRA_b, EAW49962.1 (LCOR-Cra_b) entry, where the N-terminal 111 amino acids of LCOR are fused to C10ORF12, and the two regions are separated by a 200 amino acid spacer (Figure 2C). LCOR is a ligand-dependent co-repressor interacting via its N-terminal domain with nuclear hormone receptors in a complex including CTBP and a number of histone deacetylases (Fernandes et al., 2003; Shi et al., 2003). Although our AP-MS analysis yielded peptides of the LCOR N terminus, C10ORF12 and the LCOR-CRA_b specific spacer (Figure S5C), peptides of the LCOR C terminus were missing (Figure S5D), indicating that PRC2 interacts with LCOR-CRA_b and potentially with the shorter isoform C10ORF12. To test this possibility, we performed additional AP-MS experiments using LCOR, C10ORF12, and LCOR-CRA_b as baits. LCOR purified with its known interaction partners CTBP1 and CTBP2, while PRC2 components were absent in LCOR purifications (Figures 2D and S5E). In contrast, both LCOR-CRA_b and C10ORF12 reciprocally interact with all subunits of the PCL wing of PRC2 (Figures 2B, S5D, and S5E).

To investigate the functional relevance of this finding, we employed a heterologous reporter system based on a stably integrated, constitutively active luciferase reporter gene responsive to upstream, promoter-proximal GAL4 DNA binding sites

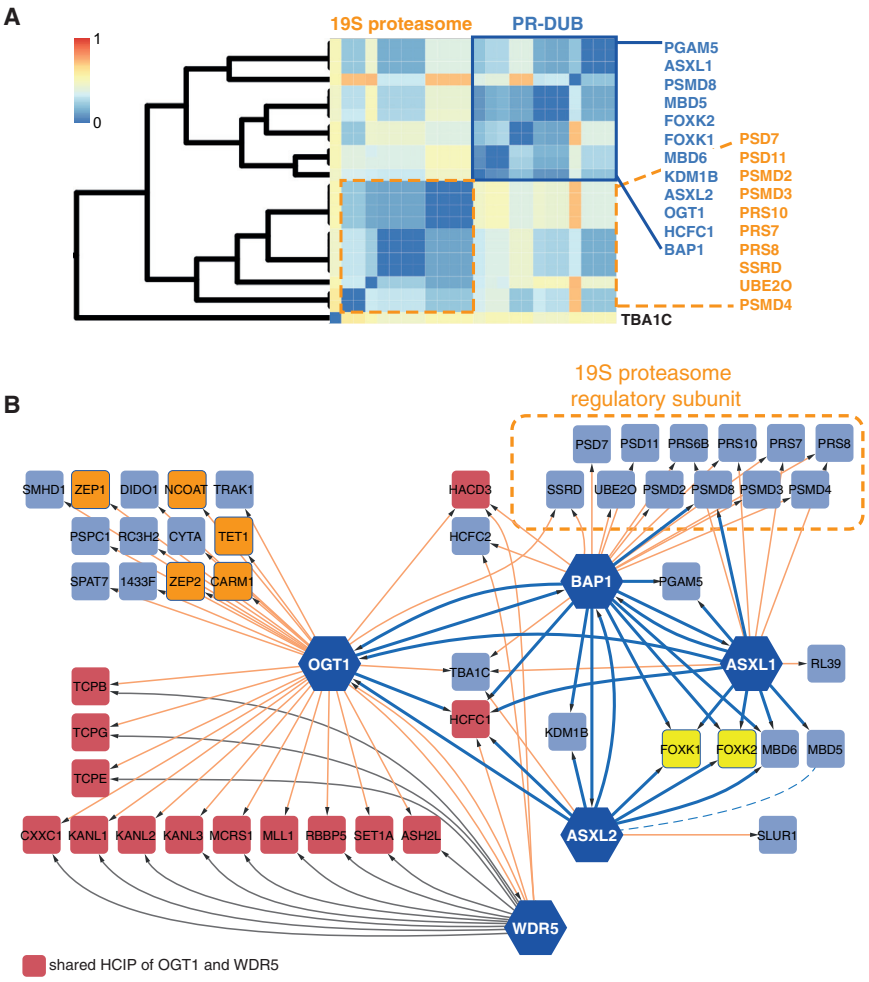

Figure 3. Human PR-DUB Complexes Contain OGT1 and FOXK Transcription Factors

(A) Excerpt of Figure 1B showing the PR-DUB and 19S proteasome clusters.

(B) Topology of PR-DUB complexes. The interactions of bait proteins with proteins localized in PR-DUB cluster are indicated in blue. WDR5 shares many interacting proteins with OGT1 (indicated in red), which are predominantly MLL/SET complex associated proteins and does not interact with BAP1, ASXL1, and 2. Hexagons: bait proteins; squares, identified HCIPs not used as baits in this study. Yellow: FOXK1 and 2. Orange nodes: OGT1 interactors. Dashed line: ASXL2-MBD5 interaction, which was detected, but did not pass our stringent filtering criteria.

(Figure 2E) (Hansen et al., 2008). We engineered cell lines containing tetracycline inducible GAL4-LCOR and GAL4-C10ORF12 expression constructs, respectively. Upon induction, both proteins accumulated in the nucleus and were recruited to the GAL4 motifs, resulting in strong repression of luciferase activity (Figures 2F–2H and S5F). To assess whether the repressive activity of C10ORF12 is mediated by recruitment of PRC2 to the target promoter, we performed chromatin immunoprecipitation (ChIP) with an H3K27me3-specific antibody and analyzed the enrichment of luciferase promoter fragments via qPCR. Upon tetracycline induction, we found that the transcription start site (TSS) of the luciferase gene was significantly trimethylated at H3K27 in the GAL4-C10ORF12 expressing cell line (Figure 2I). In contrast, despite that GAL4-LCOR was expressed at higher levels than GAL4-C10ORF12 (Figure 2F) and exhibited a 10- to 20-fold increase in its binding to the reporter (Figure 2H), no significant H3K27me3 enrichment was observed upon expression of this protein.

PCL proteins target PRC2 and positively regulate its enzymatic activity via their ability to bind methylated H3K36 (Cai et al., 2013; Musselman et al., 2012; Sarma et al., 2008). However, further experimental investigation will be required to elucidate the exact mechanism by which C17ORF96 and LCOR-CRA_b/C10ORF12 influence PRC2.1. An interesting possibility is that LCOR-CRA_b recruits PRC2.1 to nuclear hormone receptor binding sites upon ligand binding. This interaction, restricted to C10ORF12, leaves the N terminus of LCOR free for ligand responsive interaction with nuclear hormone receptors.

ASXL1 and ASXL2 Define Optional PR-DUB Complexes Containing OGT1 and FOXK Transcription Factors

The *Drosophila* PcG complex PR-DUB was identified as a heterodimer consisting of the deubiquitinase Calypso and the Asx protein (Scheuermann et al., 2010). However, the composition of its human counterpart remains elusive. Thus, we set out to systematically characterize this complex by performing purifications of BAP1, ASXL1, and ASXL2, the human homologs of the *Drosophila* PR-DUB components. Our AP-MS analysis revealed that BAP1 reciprocally interacts with both ASXL1 and ASXL2 (Figure 3B). Interestingly, the two ASXL proteins do not interact with each other (Figure 3B), suggesting the existence of two mutually exclusive PR-DUB complexes, which we called PR-DUB.1 and PR-DUB.2 depending on the ASXL partner of BAP1 being ASXL1 and ASXL2, respectively.

Both PR-DUB core components share a similar set of accessory proteins encompassing the transcription factors FOXK1 and FOXK2, the chromatin associated proteins MBD5 and MBD6, the transcriptional co-regulator HCFC1, and most notably OGT1 (Figure 3B). A recent attempt to identify BAP1 interaction partners led to the identification of Asxl1, Asxl2, Ogt, Foxk1, Kdm1b, and Hcf1 in mouse spleen tissue (Dey et al., 2012). Also, MDB5 and MBD6 have been shown to interact with BAP1 and ASXL2 in HeLa and FOXK2 with BAP1 in U2OS cells (Baymaz et al., 2014; Ji et al., 2014). Our data provide support to these results and indicate a general cell type independent

assembly of mammalian PR-DUB complexes. Furthermore, our data clearly implicate OGT1 as a member of mammalian PR-DUB complexes, an interaction which was not identified in the *Drosophila* PR-DUB complex purification (Scheuermann et al., 2010), although the *Drosophila* homolog Ogt was previously annotated as bona fide PcG protein (Gambetta et al., 2009).

OGT1 is the only O-GlcNAc transferase in mammals. The enzyme catalyzes the addition of a single GlcNAc molecule to serine and threonine of many target proteins (Hart et al., 2011). OGT1 enzymatic activity is required for mouse development and is essential for embryonic stem cell (ESC) viability (Vella et al., 2013). In addition, the protein was found to interact with BAP1 and to localize to chromatin via its interaction with the 5-methylcytosine oxidase TET1 (Dey et al., 2012; Vella et al., 2013). To further refine the connectivity of OGT1 within the PR-DUB network, we performed AP-MS experiments using OGT1 as bait.

This analysis validated the interaction between BAP1 and OGT1 and the interactions of OGT1 with TET1 and NCOAT (Figure 3B), the O-GlcNAcase counteracting OGT1 activity (Vella et al., 2013; Whisenhunt et al., 2006). Moreover, our data identified a second set of OGT1-containing complexes involved in transcriptional regulation that did not co-purify with PR-DUB core subunits (Figure 3B). These include the ZNFs ZEP1 (HIVEP1) and ZEP2 (HIVEP2) and the arginine-specific HMT CARM1. Furthermore, we identified OGT1 as a subunit of WDR5 containing complexes. Indeed, OGT1 exhibits interactions with the NSL complex and with the SET1 HMT family activating complex WDR5/RBBP5/ASH2L, which is likely to mediate the interaction of OGT1 with MLL1 and SET1A (Figure 3B). Although no interaction of OGT1 with FOXK1/2 and MBD5/6 was detected, these proteins co-cluster with PR-DUB core components and OGT1 is highly connected to the PR-DUB core (Figures 3A and 3B).

These results suggest that OGT1/HCFC1 and FOXK/MBD proteins may form optional PR-DUB.1/PR-DUB.2 complexes. Conversely, OGT1 interactions with FOXK and MBD proteins could be transient and hence difficult to pinpoint by OGT1 affinity purification.

Genomics Profiling of the FOXK1-Containing PR-DUB.1

A functional interaction of OGT1 with FOXK transcription factors within the same PR-DUB complex would require their co-localization at genomic target sites. To test this hypothesis, we examined the genome-wide distribution of O-GlcNAc, a proxy for catalytically active OGT1, ASXL1, and FOXK1 by performing chromatin immunoprecipitation followed by Next Generation Sequencing (ChIP-seq) in HEK293 cells (Figure S6A).

We found 41% and 55% of FOXK1 peaks co-localizing with O-GlcNAc and ASXL1, respectively, while 69% of O-GlcNAc peaks were co-occupied by ASXL1 (Figure 4A). In total, we identified 2,703 genomic loci bound by all three features (Figure 4A). Functional annotation of these sites to genomic compartments revealed a predominant binding of PR-DUB.1 to gene promoters (Figure 4A), with read densities sharply peaking at TSSs of RefSeq annotated genes (Figure 4B). Moreover, we found that feature enrichments within ±1 kb of TSSs are highly correlated to each other ($p > 0.8$), further indicating that ASXL1, FOXK1, and OGT1 are likely subunits of the same protein complex (Figure 4C). To identify classes of genes bound by PR-DUB.1, we subjected the set of TSSs bound by each complex member to MSigDB pathway enrichment analysis. This analysis identified highly overlapping sets of enriched pathways for each protein (Figure S6B). Notably, PR-DUB.1 targets are predominantly enriched for genes involved in fundamental cellular processes like gene expression, cell cycle, mitosis, and protein metabolism (Figure 4D).

PRC1 Complexes and PR-DUB.1 Regulate Different Target Genes

Mutations in *Drosophila sxc* (the gene encoding Ogt), *calypso*, and *Asx* genes lead to derepression of HOX genes, and previous studies reported a strong co-localization of PR-DUB and O-GlcNAc with major PRC1 bound sites at inactive genes in *Drosophila* (Gambetta et al., 2009; Scheuermann et al., 2010). We sought to investigate this relation in the human genome by comparing our PR-DUB profiles with publicly available ChIP-seq data of RING2 and RYBP (Gao et al., 2012), as well as TIF1B (Iyengar et al., 2011).

Our analysis therefore focused on six representatives of the three major modules within our PcG interaction network at the chromatin level: RING2 and RYBP, the central core of the PRC1 module (Figure 1C), TIF1B, the common component of ZNFs containing CBX1/3/5 complexes (Figure S4A), and PR-DUB.1. Besides the expected high correlation between RING2 and RYBP ($p = 0.78$; Figure S6C), pairwise correlation analysis of feature enrichments at promoters revealed a clear segregation between PRC1 and TIF1B on the one hand and PR-DUB.1 on the other hand (Figures 4E, 4F, and S6C). Similarly, when comparing the genome-wide distribution of PR-DUB.1 (2,703 ASXL1+GlcNAc+FOXK1 co-occupied regions) with "PRC1" (6,816 RING2+RYBP peaks) and TIF1B (10,297 peaks), we observed only a partial co-localization of these three complexes at target sites, with 24% and 31% of PR-DUB.1 binding sites co-bound by PRC1 and TIF1B, respectively, and only 336 regions occupied by all three complexes (Figure 4F).

In summary, our analysis uncovered the basic topology of the human PR-DUB network at both the proteomics and genomics level. Interestingly, and in contrast to *Drosophila*, the human PR-DUB and PRC1 complexes bind largely distinct sets of target genes, strongly suggesting they are involved in different cellular processes in mammals. In addition, our AP-MS experiments identified the transcription factors FOXK1 and FOXK2 as components of PR-DUB, hence highlighting a potential recruitment mechanism of PR-DUB complexes and supporting recent findings that FOXK2 can specifically target BAP1 to chromatin (Ji et al., 2014). We anticipate that future experiments based on our data will shed light on the functionality of PR-DUB complexes in gene regulation and their relation to PRC1 and PRC2.

Conclusions

Although considerable progress has been made in determining the composition of mammalian PcG protein complexes, recent findings are primarily based on studies of isolated protein components in different cellular contexts with heterogeneous

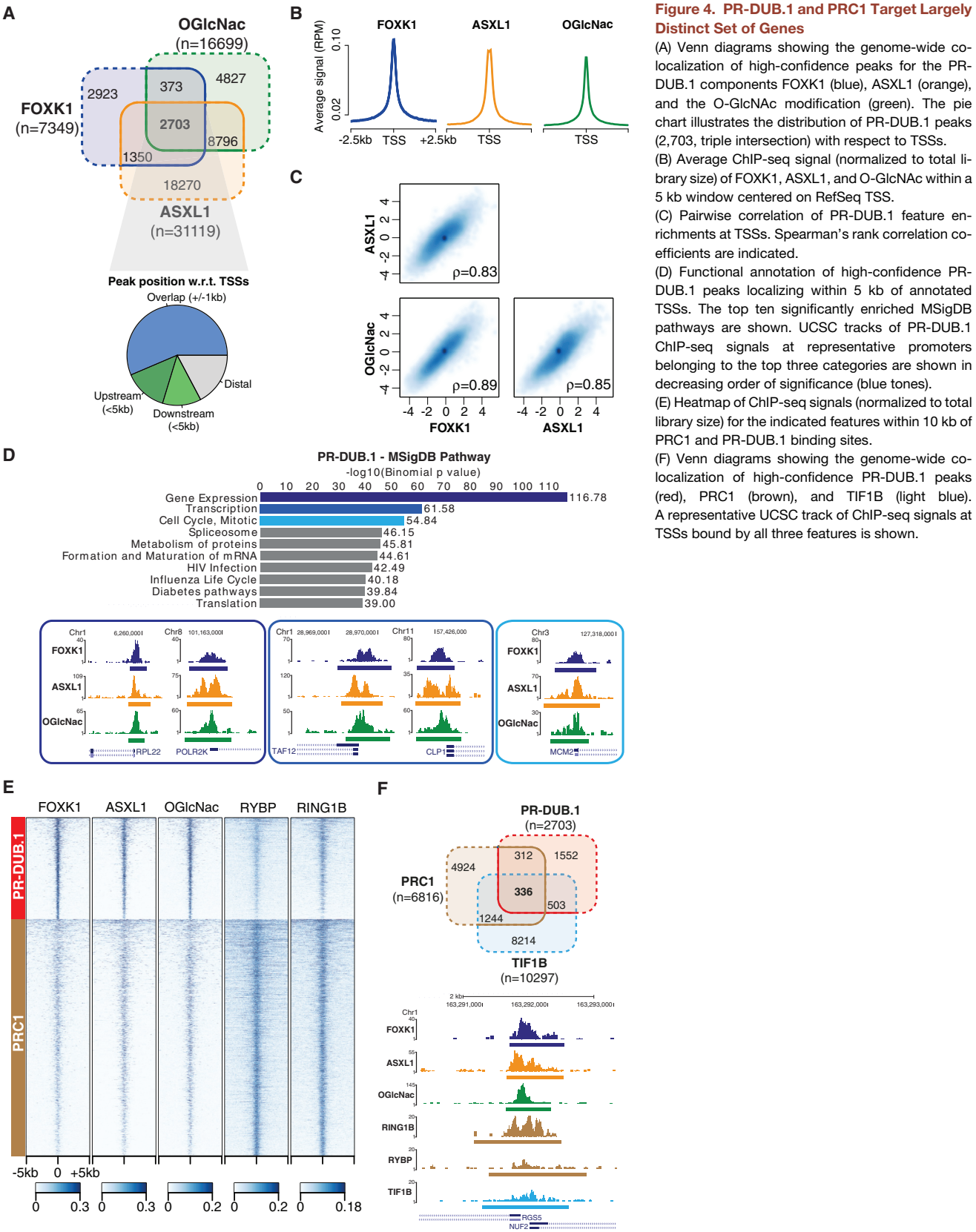

Figure 4. PR-DUB.1 and PRC1 Target Largely Distinct Set of Genes

(A) Venn diagrams showing the genome-wide co-localization of high-confidence peaks for the PR-DUB.1 components FOXK1 (blue), ASXL1 (orange), and the O-GlcNAc modification (green). The pie chart illustrates the distribution of PR-DUB.1 peaks (2,703, triple intersection) with respect to TSSs.

(B) Average ChIP-seq signal (normalized to total library size) of FOXK1, ASXL1, and O-GlcNAc within a 5 kb window centered on RefSeq TSS.

(C) Pairwise correlation of PR-DUB.1 feature enrichments at TSSs. Spearman's rank correlation coefficients are indicated.

(D) Functional annotation of high-confidence PR-DUB.1 peaks localizing within 5 kb of annotated TSSs. The top ten significantly enriched MSigDB pathways are shown. UCSC tracks of PR-DUB.1 ChIP-seq signals at representative promoters belonging to the top three categories are shown in decreasing order of significance (blue tones).

(E) Heatmap of ChIP-seq signals (normalized to total library size) for the indicated features within 10 kb of PRC1 and PR-DUB.1 binding sites.

(F) Venn diagrams showing the genome-wide co-localization of high-confidence PR-DUB.1 peaks (red), PRC1 (brown), and TIF1B (light blue). A representative UCSC track of ChIP-seq signals at TSSs bound by all three features is shown.

biochemical workflows, thus hampering a system-level understanding of gene silencing. In this study, in contrast, we used a systematic proteomic approach to comprehensively map the PcG protein interactome in a single human cell line. Since the abundance of PcG proteins can vary between cell types and surely influences the assembly of alternative protein complexes, we chose HEK293 cells for our study as all PcG proteins are expressed in this cell type. The result is a high-density interaction network, which enabled us to dissect individual PcG complexes with unprecedented detail. By allocating newly identified interaction partners to all PcG complex families and by identifying candidate subunits responsible for complex targeting to chromatin, we obtained insights into molecular function and recruitment of the PcG silencing system.

In addition to the fine mapping of the cardinal PcG complexes PRC1 and PRC2, our data unravel human PR-DUB as a multifaceted assembly comprising OGT1 along with several transcription and chromatin binding factors. Therefore, our study testifies the significant diversity that exists among individual PcG complexes in a single cell line. In addition, it provides a solid framework for future systematic experiments aiming at disentangling the biochemistry of PcG protein-mediated gene regulation in mammalian cells.

EXPERIMENTAL PROCEDURES

Expression Constructs and Generation of Stable Cell Lines

To generate expression vectors for tetracycline-induced expression of N-terminally SH-tagged bait proteins, human open reading frames (ORFs) within pDONR223 vectors were picked from a Gateway-compatible human orfeome collection (HORFeome v5.1, Open Biosystems) for LR recombination with the customized destination vector pcDNA5/FRT/TO/SH/GW, which was obtained through ligation of the SH-tag coding sequence and the Gateway recombination cassette into the polylinker of pcDNA5/FTR/TO (Invitrogen). Genes not in the human orfeome collection were amplified from human cDNA prepared from HEK293 cells by PCR and cloned into entry vectors by TOPO (pENTR/D-TOPO) reaction. Stable Flp-In HEK293 T-REx cell lines were generated as described in the Supplemental Information.

Protein Purification

Stable Flp-In HEK293 T-REx cell lines were grown in five 14.5 cm Greiner dishes to 80% confluency and bait protein expression induced by the addition of 1 μg/mL of tetracycline to the medium 16–24 hr prior to harvest in PBS containing 1 mM EDTA. The suspended cells were pelleted and drained from the supernatant for subsequent shock freezing in liquid nitrogen and long-term storage at −80°C.

The frozen cell pellets were resuspended in 5 mL TNN lysis buffer (100 mM Tris [pH 8.0], 5 mM ETDA, 250 mM NaCl, 50 mM NaF, 1% Igepal CA-630 [Nonidet P-40 Substitute], 1.5 mM Na3VO4, 1 mM PMSF, 1 mM DTT, and 1× Protease Inhibitor mix [Roche]) and rested on ice for 10 min. Insolubilizable material was removed by centrifugation. Cleared lysates were loaded on a pre-equilibrated spin column (Bio-Rad) containing 200 μL Strep-Tactin Sepharose (IBA BioTAGnology). The Sepharose was washed four times with 1 mL TNN lysis buffer (Igepal CA-630 and DTT concentrations adjusted to 0.5% and 0.5 mM, respectively). Bound proteins were eluted with 1 mL 2 mM biotin in TNN lysis buffer (Igepal CA-630 and DTT concentrations adjusted to 0.5% and 0.5 mM, respectively), incubated for 2 hr with 100 μL HA-Agarose (Sigma), washed four times with TNN lysis buffer (Igepal CA-630 concentration adjusted to 0.5%, w/o DTT and w/o protease inhibitors), and two additional times in TNN buffer (100 mM Tris pH 8.0, 150 mM NaCl, and 50 mM NaF). The bound proteins were released by acidic elution with 500 μL 0.2 M Glycine pH 2.5 and the eluate was pH neutralized with NH_4HCO_3. Cysteine bonds were reduced with 5 mM TCEP for 30 min at 37°C and alkylated in 10 mM iodacetamide for 20 min at room temperature in the dark. Samples were digested with 1 μg trypsin (Promega) overnight at 37°C.

Bait proteins with low protein yield were processed by single step purification, omitting the HA step. The frozen cell pellets were resuspended in 5 mL of TNN lysis buffer containing 10 μg/mL avidin. The eluates were TCA precipitated to remove biotin and resolubilized in 50 μL 10% ACN, 50 mM NH_4HCO_3 pH 8.8. After dilution with NH_4HCO_3 to 5% ACN, the samples were reduced, alkylated, and digested as in the double step protocol.

The digested peptides were purified with C18 MicroSpin columns (The Nest Group) according to the protocol of the manufacturer, resolved in 0.1% formic acid, and 1% acetonitrile for mass spectrometry analysis.

Mass Spectrometry

LC-MS/MS analysis was performed on an LTQ Orbitrap XL mass spectrometer (Thermo Fisher Scientific). Peptide separation was carried out by reverse phase on a Proxeon EASY-nLC II liquid chromatography system (Thermo Fisher Scientific). The reverse phase column (75 μm × 10 cm) was packed with Magic C18 AQ (3 μm) resin (WICOM International). A linear gradient from 5% to 35% acetonitrile in 0.1% formic acid was run for 60 min at a flow rate of 300 nL/min. Data acquisition was set to obtain one high resolution MS scan in the Orbitrap (60,000 at 400 m/z) followed by six collision-induced fragmentation (CID) MS/MS fragment ion spectra in the linear trap quadrupole (LTQ). Orbitrap charge state screening was enabled and ions with unassigned or single charge states were rejected. The dynamic exclusion window was set to 15 s and limited to 300 entries. The minimal precursor ion current to trigger CID and MS/MS scan was set to 150. The ion accumulation time was set to 500 ms (MS) and 250 ms (MS/MS) using a target setting of 10^6 (MS) and 10^4 (MS/MS) ions. After every replicate series, a peptide reference sample containing 200 fmol of human [Glu1]-Fibrinopeptide B (Sigma-Aldrich) was analyzed to monitor the overall LC-MS/MS systems performance.

ChIP and Preparation of ChIP-Seq Libraries

Chromatin fixation and immunoprecipitation were performed essentially as described (Orlando et al., 1997). Cells (3–4 × 10^8) were fixed in 200 mL of medium with 1% formaldehyde for 10 min at room temperature. Cross-linked cells were sonicated to produce chromatin fragments of an average size of 150–400 bp. Soluble chromatin was separated from insoluble material by centrifugation. The supernatant containing chromatin of 1–2 × 10^7 cells was used for immunoprecipitation. Sequencing libraries were prepared with the NEB Genomic DNA Sample Preparation Kit according to NEB's instructions. After adaptor ligation, library fragments of 250–350 bp were isolated from an agarose gel. The DNA was PCR amplified with Illumina primers with 18 cycles, purified, and loaded on an Illumina flow cell for cluster generation. Libraries were sequenced on the Genome Analyzer IIx (TrueSeq cBot-GA v2 and TruSeq v5 SBS Kit) and HiSeq 2000 (HiSeq Flow Cell v3 and TruSeq SBS Kit v3) following the manufacturer's protocols.

For ChIP-qPCR, nuclei were prepared essentially as described in "Functional Analysis of DNA and Chromatin" (Santoro, 2014). Immunoprecipitations were performed using Anti-GAL4 (sc-510, Santa Cruz Biotechnology), Anti-IgG (10500C, Invitrogen), and Anti-H3K27me3 kindly provided by Thomas Jenuwein. Anti-FOXK1 (ab18196) was purchased from Abcam, Anti-ASXL1 (sc85283) from Santa Cruz Biotechnology, and Anti-GlcNAc (HGAC85) from Novus Biologicals. Primer sets used for qPCR are listed in the Supplemental Information.

Data Analysis

Description of data processing and analysis methods are available in the Supplemental Information.

ACCESSION NUMBERS

The accession numbers for the mass spectrometry, protein interactions, and sequencing data reported in this paper are PeptideAtlas: PASS00347; IntAct: IM-21659 (Orchard et al., 2014); and GEO: GSE51673, respectively.

SUPPLEMENTAL INFORMATION

Supplemental Information includes Supplemental Experimental Procedures, six figures, and three tables and can be found with this article online at http://dx.doi.org/10.1016/j.celrep.2016.08.096.

AUTHOR CONTRIBUTIONS

C.B., M. Gstaiger, F.C., and S.H. designed the study. S.H., F.C., M.S., C.B., and T.G. carried out the experiments. S.H. performed the mass spectrometric measurements and analysis. S.H. and F.C. analyzed the interaction data. F.C. and M. Gerstung performed the genomics data analysis. T.G. and K.H. provided reagents and protocols. F.C., S.H., C.B., M. Gstaiger, R.A., and R.P. wrote the manuscript.

ACKNOWLEDGMENTS

We thank I. Nissen and M. Kohler for technical support on ChIP-seq and U. Nussbaumer for excellent technical support on the implementation of the AP workflow. Illumina sequencing was done in the Genomics Facility Basel at D-BSSE, ETH Zurich. Research of S.H. and M. Gstaiger is supported by the European Union 7th Framework Programme SYBILLA (Systems Biology of T-Cell Activation) and the Innovative Medicines Initiative project ULTRA-DD. R.A.'s research is funded by advanced ERC grant Proteomics v3.0 (233226) and by SystemsX.ch, the Swiss initiative for systems biology. R.P.'s research is funded by Epigenesys, the Swiss National Science Foundation, and the ETH Zurich. C.B.'s research is funded by SystemsX.ch, the Swiss initiative for systems biology.

Received: July 29, 2016
Revised: August 23, 2016
Accepted: August 30, 2016
Published: October 4, 2016

REFERENCES

Alekseyenko, A.A., Gorchakov, A.A., Kharchenko, P.V., and Kuroda, M.I. (2014). Reciprocal interactions of human C10orf12 and C17orf96 with PRC2 revealed by BioTAP-XL cross-linking and affinity purification. Proc. Natl. Acad. Sci. USA *111*, 2488–2493.

Baymaz, H.I., Fournier, A., Laget, S., Ji, Z., Jansen, P.W., Smits, A.H., Ferry, L., Mensinga, A., Poser, I., Sharrocks, A., et al. (2014). MBD5 and MBD6 interact with the human PR-DUB complex through their methyl-CpG-binding domain. Proteomics *14*, 2179–2189.

Behrends, C., Sowa, M.E., Gygi, S.P., and Harper, J.W. (2010). Network organization of the human autophagy system. Nature *466*, 68–76.

Beisel, C., and Paro, R. (2011). Silencing chromatin: comparing modes and mechanisms. Nat. Rev. Genet. *12*, 123–135.

Bernstein, E., Duncan, E.M., Masui, O., Gil, J., Heard, E., and Allis, C.D. (2006). Mouse polycomb proteins bind differentially to methylated histone H3 and RNA and are enriched in facultative heterochromatin. Mol. Cell. Biol. *26*, 2560–2569.

Cai, Y., Jin, J., Swanson, S.K., Cole, M.D., Choi, S.H., Florens, L., Washburn, M.P., Conaway, J.W., and Conaway, R.C. (2010). Subunit composition and substrate specificity of a MOF-containing histone acetyltransferase distinct from the male-specific lethal (MSL) complex. J. Biol. Chem. *285*, 4268–4272.

Cai, L., Rothbart, S.B., Lu, R., Xu, B., Chen, W.Y., Tripathy, A., Rockowitz, S., Zheng, D., Patel, D.J., Allis, C.D., et al. (2013). An H3K36 methylation-engaging Tudor motif of polycomb-like proteins mediates PRC2 complex targeting. Mol. Cell *49*, 571–582.

Cao, R., Wang, L., Wang, H., Xia, L., Erdjument-Bromage, H., Tempst, P., Jones, R.S., and Zhang, Y. (2002). Role of histone H3 lysine 27 methylation in Polycomb-group silencing. Science *298*, 1039–1043.

Caubit, X., Thangarajah, R., Theil, T., Wirth, J., Nothwang, H.G., Rüther, U., and Krauss, S. (1999). Mouse Dac, a novel nuclear factor with homology to Drosophila dachshund shows a dynamic expression in the neural crest, the eye, the neocortex, and the limb bud. Dev. Dyn. *214*, 66–80.

Craig, R., and Beavis, R.C. (2004). TANDEM: matching proteins with tandem mass spectra. Bioinformatics *20*, 1466–1467.

de Napoles, M., Mermoud, J.E., Wakao, R., Tang, Y.A., Endoh, M., Appanah, R., Nesterova, T.B., Silva, J., Otte, A.P., Vidal, M., et al. (2004). Polycomb group proteins Ring1A/B link ubiquitylation of histone H2A to heritable gene silencing and X inactivation. Dev. Cell *7*, 663–676.

Deutsch, E.W., Mendoza, L., Shteynberg, D., Farrah, T., Lam, H., Tasman, N., Sun, Z., Nilsson, E., Pratt, B., Prazen, B., et al. (2010). A guided tour of the Trans-Proteomic Pipeline. Proteomics *10*, 1150–1159.

Dey, A., Seshasayee, D., Noubade, R., French, D.M., Liu, J., Chaurushiya, M.S., Kirkpatrick, D.S., Pham, V.C., Lill, J.R., Bakalarski, C.E., et al. (2012). Loss of the tumor suppressor BAP1 causes myeloid transformation. Science *337*, 1541–1546.

Dietrich, N., Lerdrup, M., Landt, E., Agrawal-Singh, S., Bak, M., Tommerup, N., Rappsilber, J., Södersten, E., and Hansen, K. (2012). REST-mediated recruitment of polycomb repressor complexes in mammalian cells. PLoS Genet. *8*, e1002494.

Dou, Y., Milne, T.A., Ruthenburg, A.J., Lee, S., Lee, J.W., Verdine, G.L., Allis, C.D., and Roeder, R.G. (2006). Regulation of MLL1 H3K4 methyltransferase activity by its core components. Nat. Struct. Mol. Biol. *13*, 713–719.

El Messaoudi-Aubert, S., Nicholls, J., Maertens, G.N., Brookes, S., Bernstein, E., and Peters, G. (2010). Role for the MOV10 RNA helicase in polycomb-mediated repression of the INK4a tumor suppressor. Nat. Struct. Mol. Biol. *17*, 862–868.

Enderle, D., Beisel, C., Stadler, M.B., Gerstung, M., Athri, P., and Paro, R. (2011). Polycomb preferentially targets stalled promoters of coding and noncoding transcripts. Genome Res. *21*, 216–226.

Farcas, A.M., Blackledge, N.P., Sudbery, I., Long, H.K., McGouran, J.F., Rose, N.R., Lee, S., Sims, D., Cerase, A., Sheahan, T.W., et al. (2012). KDM2B links the Polycomb Repressive Complex 1 (PRC1) to recognition of CpG islands. eLife *1*, e00205.

Fernandes, I., Bastien, Y., Wai, T., Nygard, K., Lin, R., Cormier, O., Lee, H.S., Eng, F., Bertos, N.R., Pelletier, N., et al. (2003). Ligand-dependent nuclear receptor corepressor LCoR functions by histone deacetylase-dependent and -independent mechanisms. Mol. Cell *11*, 139–150.

Fischle, W., Wang, Y., Jacobs, S.A., Kim, Y., Allis, C.D., and Khorasanizadeh, S. (2003). Molecular basis for the discrimination of repressive methyl-lysine marks in histone H3 by Polycomb and HP1 chromodomains. Genes Dev. *17*, 1870–1881.

Furuyama, T., Banerjee, R., Breen, T.R., and Harte, P.J. (2004). SIR2 is required for polycomb silencing and is associated with an E(Z) histone methyltransferase complex. Curr. Biol. *14*, 1812–1821.

Gambetta, M.C., Oktaba, K., and Müller, J. (2009). Essential role of the glycosyltransferase sxc/Ogt in polycomb repression. Science *325*, 93–96.

Gao, Z., Zhang, J., Bonasio, R., Strino, F., Sawai, A., Parisi, F., Kluger, Y., and Reinberg, D. (2012). PCGF homologs, CBX proteins, and RYBP define functionally distinct PRC1 family complexes. Mol. Cell *45*, 344–356.

Glatter, T., Wepf, A., Aebersold, R., and Gstaiger, M. (2009). An integrated workflow for charting the human interaction proteome: insights into the PP2A system. Mol. Syst. Biol. *5*, 237.

Hansen, K.H., Bracken, A.P., Pasini, D., Dietrich, N., Gehani, S.S., Monrad, A., Rappsilber, J., Lerdrup, M., and Helin, K. (2008). A model for transmission of the H3K27me3 epigenetic mark. Nat. Cell Biol. *10*, 1291–1300.

Hart, G.W., Slawson, C., Ramirez-Correa, G., and Lagerlof, O. (2011). Cross talk between O-GlcNAcylation and phosphorylation: roles in signaling, transcription, and chronic disease. Annu. Rev. Biochem. *80*, 825–858.

He, J., Shen, L., Wan, M., Taranova, O., Wu, H., and Zhang, Y. (2013). Kdm2b maintains murine embryonic stem cell status by recruiting PRC1 complex to CpG islands of developmental genes. Nat. Cell Biol. *15*, 373–384.

Hunkapiller, J., Shen, Y., Diaz, A., Cagney, G., McCleary, D., Ramalho-Santos, M., Krogan, N., Ren, B., Song, J.S., and Reiter, J.F. (2012). Polycomb-like

3 promotes polycomb repressive complex 2 binding to CpG islands and embryonic stem cell self-renewal. PLoS Genet. *8*, e1002576.

Iyengar, S., Ivanov, A.V., Jin, V.X., Rauscher, F.J., 3rd, and Farnham, P.J. (2011). Functional analysis of KAP1 genomic recruitment. Mol. Cell. Biol. *31*, 1833–1847.

Jaenisch, R., and Young, R. (2008). Stem cells, the molecular circuitry of pluripotency and nuclear reprogramming. Cell *132*, 567–582.

Ji, Z., Mohammed, H., Webber, A., Ridsdale, J., Han, N., Carroll, J.S., and Sharrocks, A.D. (2014). The forkhead transcription factor FOXK2 acts as a chromatin targeting factor for the BAP1-containing histone deubiquitinase complex. Nucleic Acids Res. *42*, 6232–6242.

Junco, S.E., Wang, R., Gaipa, J.C., Taylor, A.B., Schirf, V., Gearhart, M.D., Bardwell, V.J., Demeler, B., Hart, P.J., and Kim, C.A. (2013). Structure of the polycomb group protein PCGF1 in complex with BCOR reveals basis for binding selectivity of PCGF homologs. Structure *21*, 665–671.

Kalb, R., Latwiel, S., Baymaz, H.I., Jansen, P.W., Müller, C.W., Vermeulen, M., and Müller, J. (2014). Histone H2A monoubiquitination promotes histone H3 methylation in Polycomb repression. Nat. Struct. Mol. Biol. *21*, 569–571.

Kim, T.G., Kraus, J.C., Chen, J., and Lee, Y. (2003). JUMONJI, a critical factor for cardiac development, functions as a transcriptional repressor. J. Biol. Chem. *278*, 42247–42255.

Kim, H., Kang, K., and Kim, J. (2009). AEBP2 as a potential targeting protein for Polycomb Repression Complex PRC2. Nucleic Acids Res. *37*, 2940–2950.

Klymenko, T., Papp, B., Fischle, W., Köcher, T., Schelder, M., Fritsch, C., Wild, B., Wilm, M., and Müller, J. (2006). A Polycomb group protein complex with sequence-specific DNA-binding and selective methyl-lysine-binding activities. Genes Dev. *20*, 1110–1122.

Lagarou, A., Mohd-Sarip, A., Moshkin, Y.M., Chalkley, G.E., Bezstarosti, K., Demmers, J.A., and Verrijzer, C.P. (2008). dKDM2 couples histone H2A ubiquitylation to histone H3 demethylation during Polycomb group silencing. Genes Dev. *22*, 2799–2810.

Maier, V.K., Feeney, C.M., Taylor, J.E., Creech, A.L., Qiao, J.W., Szanto, A., Das, P.P., Chevrier, N., Cifuentes-Rojas, C., Orkin, S.H., et al. (2015). Functional proteomic analysis of repressive histone methyltransferase complexes reveals ZNF518B as a G9A regulator. Mol. Cell. Proteomics *14*, 1435–1446.

Margueron, R., and Reinberg, D. (2011). The Polycomb complex PRC2 and its mark in life. Nature *469*, 343–349.

Margueron, R., Li, G., Sarma, K., Blais, A., Zavadil, J., Woodcock, C.L., Dynlacht, B.D., and Reinberg, D. (2008). Ezh1 and Ezh2 maintain repressive chromatin through different mechanisms. Mol. Cell *32*, 503–518.

Maurange, C., Lee, N., and Paro, R. (2006). Signaling meets chromatin during tissue regeneration in Drosophila. Curr. Opin. Genet. Dev. *16*, 485–489.

Migliori, V., Mapelli, M., and Guccione, E. (2012). On WD40 proteins: propelling our knowledge of transcriptional control? Epigenetics *7*, 815–822.

Min, J., Zhang, Y., and Xu, R.M. (2003). Structural basis for specific binding of Polycomb chromodomain to histone H3 methylated at Lys 27. Genes Dev. *17*, 1823–1828.

Miyata, Y., and Nishida, E. (2011). DYRK1A binds to an evolutionarily conserved WD40-repeat protein WDR68 and induces its nuclear translocation. Biochim. Biophys. Acta *1813*, 1728–1739.

Morey, L., Pascual, G., Cozzuto, L., Roma, G., Wutz, A., Benitah, S.A., and Di Croce, L. (2012). Nonoverlapping functions of the Polycomb group Cbx family of proteins in embryonic stem cells. Cell Stem Cell *10*, 47–62.

Müller, J., Hart, C.M., Francis, N.J., Vargas, M.L., Sengupta, A., Wild, B., Miller, E.L., O'Connor, M.B., Kingston, R.E., and Simon, J.A. (2002). Histone methyltransferase activity of a Drosophila Polycomb group repressor complex. Cell *111*, 197–208.

Musselman, C.A., Avvakumov, N., Watanabe, R., Abraham, C.G., Lalonde, M.E., Hong, Z., Allen, C., Roy, S., Nuñez, J.K., Nickoloff, J., et al. (2012). Molecular basis for H3K36me3 recognition by the Tudor domain of PHF1. Nat. Struct. Mol. Biol. *19*, 1266–1272.

Ogawa, H., Ishiguro, K., Gaubatz, S., Livingston, D.M., and Nakatani, Y. (2002). A complex with chromatin modifiers that occupies E2F- and Myc-responsive genes in G0 cells. Science *296*, 1132–1136.

Oktaba, K., Gutiérrez, L., Gagneur, J., Girardot, C., Sengupta, A.K., Furlong, E.E., and Müller, J. (2008). Dynamic regulation by polycomb group protein complexes controls pattern formation and the cell cycle in Drosophila. Dev. Cell *15*, 877–889.

Orchard, S., Ammari, M., Aranda, B., Breuza, L., Briganti, L., Broackes-Carter, F., Campbell, N.H., Chavali, G., Chen, C., del-Toro, N., et al. (2014). The MIntAct project–IntAct as a common curation platform for 11 molecular interaction databases. Nucleic Acids Res. *42*, D358–D363.

Orlando, V., Strutt, H., and Paro, R. (1997). Analysis of chromatin structure by in vivo formaldehyde cross-linking. Methods *11*, 205–214.

Pasini, D., Cloos, P.A., Walfridsson, J., Olsson, L., Bukowski, J.P., Johansen, J.V., Bak, M., Tommerup, N., Rappsilber, J., and Helin, K. (2010). JARID2 regulates binding of the Polycomb repressive complex 2 to target genes in ES cells. Nature *464*, 306–310.

Peng, J.C., Valouev, A., Swigut, T., Zhang, J., Zhao, Y., Sidow, A., and Wysocka, J. (2009). Jarid2/Jumonji coordinates control of PRC2 enzymatic activity and target gene occupancy in pluripotent cells. Cell *139*, 1290–1302.

Qin, J., Whyte, W.A., Anderssen, E., Apostolou, E., Chen, H.H., Akbarian, S., Bronson, R.T., Hochedlinger, K., Ramaswamy, S., Young, R.A., and Hock, H. (2012). The polycomb group protein L3mbtl2 assembles an atypical PRC1-family complex that is essential in pluripotent stem cells and early development. Cell Stem Cell *11*, 319–332.

Ringrose, L. (2007). Polycomb comes of age: genome-wide profiling of target sites. Curr. Opin. Cell Biol. *19*, 290–297.

Sánchez, C., Sánchez, I., Demmers, J.A., Rodriguez, P., Strouboulis, J., and Vidal, M. (2007). Proteomics analysis of Ring1B/Rnf2 interactors identifies a novel complex with the Fbxl10/Jhdm1B histone demethylase and the Bcl6 interacting corepressor. Mol. Cell. Proteomics *6*, 820–834.

Sanchez-Pulido, L., Devos, D., Sung, Z.R., and Calonje, M. (2008). RAWUL: a new ubiquitin-like domain in PRC1 ring finger proteins that unveils putative plant and worm PRC1 orthologs. BMC Genomics *9*, 308.

Santoro, R. (2014). Analysis of chromatin composition of repetitive sequences: the ChIP-Chop assay. Methods Mol. Biol. *1094*, 319–328.

Sarkies, P., and Sale, J.E. (2012). Cellular epigenetic stability and cancer. Trends Genet. *28*, 118–127.

Sarma, K., Margueron, R., Ivanov, A., Pirrotta, V., and Reinberg, D. (2008). Ezh2 requires PHF1 to efficiently catalyze H3 lysine 27 trimethylation in vivo. Mol. Cell. Biol. *28*, 2718–2731.

Saurin, A.J., Shao, Z., Erdjument-Bromage, H., Tempst, P., and Kingston, R.E. (2001). A Drosophila Polycomb group complex includes Zeste and dTAFII proteins. Nature *412*, 655–660.

Scheuermann, J.C., de Ayala Alonso, A.G., Oktaba, K., Ly-Hartig, N., McGinty, R.K., Fraterman, S., Wilm, M., Muir, T.W., and Müller, J. (2010). Histone H2A deubiquitinase activity of the Polycomb repressive complex PR-DUB. Nature *465*, 243–247.

Schuettengruber, B., Ganapathi, M., Leblanc, B., Portoso, M., Jaschek, R., Tolhuis, B., van Lohuizen, M., Tanay, A., and Cavalli, G. (2009). Functional anatomy of polycomb and trithorax chromatin landscapes in Drosophila embryos. PLoS Biol. *7*, e13.

Shen, X., Liu, Y., Hsu, Y.J., Fujiwara, Y., Kim, J., Mao, X., Yuan, G.C., and Orkin, S.H. (2008). EZH1 mediates methylation on histone H3 lysine 27 and complements EZH2 in maintaining stem cell identity and executing pluripotency. Mol. Cell *32*, 491–502.

Shen, X., Kim, W., Fujiwara, Y., Simon, M.D., Liu, Y., Mysliwiec, M.R., Yuan, G.C., Lee, Y., and Orkin, S.H. (2009). Jumonji modulates polycomb activity and self-renewal versus differentiation of stem cells. Cell *139*, 1303–1314.

Shi, Y., Sawada, J., Sui, G., Affar, B., Whetstine, J.R., Lan, F., Ogawa, H., Luke, M.P., Nakatani, Y., and Shi, Y. (2003). Coordinated histone modifications mediated by a CtBP co-repressor complex. Nature *422*, 735–738.

Smits, A.H., Jansen, P.W., Poser, I., Hyman, A.A., and Vermeulen, M. (2013). Stoichiometry of chromatin-associated protein complexes revealed by label-free quantitative mass spectrometry-based proteomics. Nucleic Acids Res. *41*, e28.

Sparmann, A., and van Lohuizen, M. (2006). Polycomb silencers control cell fate, development and cancer. Nat. Rev. Cancer *6*, 846–856.

Stock, J.K., Giadrossi, S., Casanova, M., Brookes, E., Vidal, M., Koseki, H., Brockdorff, N., Fisher, A.G., and Pombo, A. (2007). Ring1-mediated ubiquitination of H2A restrains poised RNA polymerase II at bivalent genes in mouse ES cells. Nat. Cell Biol. *9*, 1428–1435.

Strübbe, G., Popp, C., Schmidt, A., Pauli, A., Ringrose, L., Beisel, C., and Paro, R. (2011). Polycomb purification by in vivo biotinylation tagging reveals cohesin and Trithorax group proteins as interaction partners. Proc. Natl. Acad. Sci. USA *108*, 5572–5577.

Tavares, L., Dimitrova, E., Oxley, D., Webster, J., Poot, R., Demmers, J., Bezstarosti, K., Taylor, S., Ura, H., Koide, H., et al. (2012). RYBP-PRC1 complexes mediate H2A ubiquitylation at polycomb target sites independently of PRC2 and H3K27me3. Cell *148*, 664–678.

Trojer, P., Cao, A.R., Gao, Z., Li, Y., Zhang, J., Xu, X., Li, G., Losson, R., Erdjument-Bromage, H., Tempst, P., et al. (2011). L3MBTL2 protein acts in concert with PcG protein-mediated monoubiquitination of H2A to establish a repressive chromatin structure. Mol. Cell *42*, 438–450.

van den Boom, V., Rozenveld-Geugien, M., Bonardi, F., Malanga, D., van Gosliga, D., Heijink, A.M., Viglietto, G., Morrone, G., Fusetti, F., Vellenga, E., and Schuringa, J.J. (2013). Nonredundant and locus-specific gene repression functions of PRC1 paralog family members in human hematopoietic stem/progenitor cells. Blood *121*, 2452–2461.

van den Boom, V., Maat, H., Geugien, M., Rodríguez López, A., Sotoca, A.M., Jaques, J., Brouwers-Vos, A.Z., Fusetti, F., Groen, R.W., Yuan, H., et al. (2016). Non-canonical PRC1.1 targets active genes independent of H3K27me3 and is essential for leukemogenesis. Cell Rep. *14*, 332–346.

Vandamme, J., Völkel, P., Rosnoblet, C., Le Faou, P., and Angrand, P.O. (2011). Interaction proteomics analysis of polycomb proteins defines distinct PRC1 complexes in mammalian cells. Mol. Cell. Proteomics *10*, 002642.

Varjosalo, M., Sacco, R., Stukalov, A., van Drogen, A., Planyavsky, M., Hauri, S., Aebersold, R., Bennett, K.L., Colinge, J., Gstaiger, M., and Superti-Furga, G. (2013). Interlaboratory reproducibility of large-scale human protein-complex analysis by standardized AP-MS. Nat. Methods *10*, 307–314.

Vella, P., Scelfo, A., Jammula, S., Chiacchiera, F., Williams, K., Cuomo, A., Roberto, A., Christensen, J., Bonaldi, T., Helin, K., and Pasini, D. (2013). Tet proteins connect the O-linked N-acetylglucosamine transferase Ogt to chromatin in embryonic stem cells. Mol. Cell *49*, 645–656.

Wang, H., Wang, L., Erdjument-Bromage, H., Vidal, M., Tempst, P., Jones, R.S., and Zhang, Y. (2004). Role of histone H2A ubiquitination in Polycomb silencing. Nature *431*, 873–878.

Whisenhunt, T.R., Yang, X., Bowe, D.B., Paterson, A.J., Van Tine, B.A., and Kudlow, J.E. (2006). Disrupting the enzyme complex regulating O-GlcNAcylation blocks signaling and development. Glycobiology *16*, 551–563.

Wu, K., Liu, M., Li, A., Donninger, H., Rao, M., Jiao, X., Lisanti, M.P., Cvekl, A., Birrer, M., and Pestell, R.G. (2007). Cell fate determination factor DACH1 inhibits c-Jun-induced contact-independent growth. Mol. Biol. Cell *18*, 755–767.

Wu, X., Johansen, J.V., and Helin, K. (2013). Fbxl10/Kdm2b recruits polycomb repressive complex 1 to CpG islands and regulates H2A ubiquitylation. Mol. Cell *49*, 1134–1146.

Wysocka, J., Swigut, T., Xiao, H., Milne, T.A., Kwon, S.Y., Landry, J., Kauer, M., Tackett, A.J., Chait, B.T., Badenhorst, P., et al. (2006). A PHD finger of NURF couples histone H3 lysine 4 trimethylation with chromatin remodelling. Nature *442*, 86–90.

Zhang, Z., Jones, A., Sun, C.W., Li, C., Chang, C.W., Joo, H.Y., Dai, Q., Mysliwiec, M.R., Wu, L.C., Guo, Y., et al. (2011). PRC2 complexes with JARID2, MTF2, and esPRC2p48 in ES cells to modulate ES cell pluripotency and somatic cell reprogramming. Stem Cells *29*, 229–240.

Zhang, P., Lee, H., Brunzelle, J.S., and Couture, J.F. (2012). The plasticity of WDR5 peptide-binding cleft enables the binding of the SET1 family of histone methyltransferases. Nucleic Acids Res. *40*, 4237–4246.